HHS Public Access

Author manuscript

Dev Neurobiol. Author manuscript; available in PMC 2021 March 01.

Published in final edited form as:

Dev Neurobiol. 2020 March ; 80(3-4): 85–97. doi:10.1002/dneu.22722.

Expression of a human variant of CHMP2B linked to neurodegeneration in *Drosophila* external sensory organs leads to cell fate transformations associated with increased Notch activity

Caroline Wilson[1,3,4], **Joshua Kavaler**[1,2,3], **S.Tariq Ahmad**[1,2]

[1]Colby College, Department of Biology, Waterville, ME 04901

Abstract

Proper function of cell signaling pathways is dependent upon regulated membrane trafficking events that lead to the endocytosis, recycling, and degradation of cell surface receptors. The endosomal complexes required for transport (ESCRT) genes play a critical role in the sorting of ubiquinated cell surface proteins. CHMP2B^{Intron5}, a truncated form of a human ESCRT-III protein, was discovered in a Danish family afflicted by a hereditary form of frontotemporal dementia (FTD). Although the mechanism by which the *CHMP2B* mutation in this family causes FTD is unknown, the resulting protein has been shown to disrupt normal endosomal-lysosomal pathway function and leads to aberrant regulation of signaling pathways. Here we have misexpressed CHMP2B^{Intron5} in the developing *Drosophila* external sensory (ES) organ lineage and demonstrate that it is capable of altering cell fates. Each of the cell fate transformations seen is compatible with an increase in Notch signaling. Furthermore, this interpretation is supported by evidence that expression of CHMP2B^{Intron5} in the notum environment is capable of raising the levels of Notch signaling. As such, these results add to a growing body of evidence that CHMP2B^{Intron5} can act rapidly to disrupt normal cellular function via the misregulation of critical cell surface receptor function.

Keywords

CHMP2B, frontotemporal dementia; endosomal-lysosomal pathway; *Drosophila*; bristles; *Notch*

Introduction

Regulated turnover of cell surface receptors is achieved through internalization into endosomes, fusion of endosomes into multivesicular bodies (MVBs), and targeting the

[2]co-corresponding authors: tel: 207-859-5721, fax: 207-859-5705, jkavaler@colby.edu, tel: 207-859-5722, fax: 207-859-5705, stahmad@colby.edu.

[3]These authors contributed equally to this report

[4]current address: Icahn School of Medicine at Mount Sinai, 1425 Madison Ave, Floor 9, Room 9-20, New York, NY 10029

Conflicts of Interest

The authors declare no conflict of interest.

Data Availability Statement

Data sharing is not applicable to this article as no new data were created or analyzed in this study.

MVBs to lysosomes where the cargo can be degraded (Scott, Vacca, & Gruenberg, 2014). Central to this process are the ESCRT complexes which function in cargo sorting and MVB formation. Mutations in genes encoding ESCRT proteins are associated with a wide variety of diseases, including neurodegenerative diseases such as frontotemporal dementia (FTD), amyotrophic lateral sclerosis (ALS), Huntington's disease, paraparesis, and prion disease (Stuffers, Brech, & Stenmark, 2009).

The human *CHMP2B* gene (*vps2* in yeast and *CG4618* in *Drosophila*) encodes a member of the ESCRT-III complex and mutations resulting in truncations of CHMP2B protein have been identified as the causative agent in some cases of familial neurodegenerative diseases. In one Danish family, a G-to-C mutation in the acceptor splice site of exon 6 leads to the inclusion of intron 5 in the mRNA (*CHMP2B*^{Intron5}). This transcript contains a premature stop codon and a CHMP2B protein in which the final 36 amino acids are exchanged for a single valine residue (Skibinski et al., 2005). In the case of a Belgian patient displaying familial FTD, sequence analysis uncovered a nonsense mutation that also generated a carboxyl terminus truncation of 49 amino acids (van der Zee et al., 2008). Several lines of evidence indicate that such altered proteins can exert strong effects on neuronal physiology and development via gain-of-function activity. Transgenic mice expressing CHMP2B^{Intron5} in neurons display pathological similarities to ALS and FTD (Vernay et al., 2016). Cultured mouse cortical neurons transfected with CHMP2B^{Intron5} show an accumulation of autophagosomes and exhibit increased cell death (Lee, Beigneux, Ahmad, Young, & Gao, 2007). While *CHMP2B*$^{-/-}$ mice (which possess reduced levels of CHMP2B) display normal lifespan and show no evidence of neuropathology, transgenic mice expressing CHMP2B^{Intron5} exhibit decreased survival and accumulate ubiquitin-positive inclusions in the brain (Ghazi-Noori et al., 2012). Whereas CHMP2B depletion in cultured rat hippocampal neurons decreases dendritic spine density, transfection of CHMP2B^{Intron5} into these neurons leads to increased dendritic spine density and impedes maturation of the spines (Belly et al., 2010; Chassefeyre et al., 2015). In *Drosophila*, misexpression of CHMP2B^{Intron5} targeted to the eye generates abnormal tissue growth when expressed during early eye development (Cheruiyot, Lee, Gao, & Ahmad, 2014), or melanization and neurodegeneration when expressed later specifically in photoreceptors (Ahmad, Sweeney, Lee, Sweeney, & Gao, 2009). In both cases, the phenotypes are driven by accumulation of specific cell surface receptors leading to dysregulation of the signaling pathways (the Notch pathway in the former and the Toll pathway in the latter).

In this report we have investigated the action of CHMP2B^{Intron5} in a different neurodevelopmental setting – the *Drosophila* external sensory (ES) organs, or bristles. ES organs originate from a single precursor cell (SOP or pI) which undergoes a well-characterized series of sequential divisions and cell fate specifications (summarized in Figure 1) (Lai & Orgogozo, 2004). Briefly, once the pI cell is specified, it divides to produce a pIIA and pIIB cell. The pIIB cell then divides to produce a pIII cell and a vestigial glial cell, which undergoes apoptosis. The pIIA cell divides to produce the shaft and socket cells (which generate the external bristle structures) while the pIII cell divides to produce the two internal cells – sheath cell and neuron. Asymmetries in each division arise through a combination of extrinsic mechanisms, such as cell-cell signaling via the Notch receptor pathway, and intrinsic mechanisms, such as the differential segregation of the key protein

factors like Numb, which regulates the endocytic recycling of the Notch receptor (Lai & Orgogozo, 2004; Singhania & Grueber, 2014). Mutations or manipulations in Notch pathway genes that lead to enhanced Notch signaling cause cell fate transformations toward one side of the lineage (pIIB to pIIA, shaft to socket, neuron to sheath) whereas mutations or manipulations that antagonize Notch signaling cause transformations in the opposite direction (Bang & Posakony, 1992; Hartenstein & Posakony, 1990; Parks & Muskavitch, 1993; Rhyu, Jan, & Jan, 1994; Schweisguth & Posakony, 1994).

We show that expression of CHMP2B^{Intron5} during the development of the ES organ lineage has profound effects on cell fate specification, leading to the transformation of several cell types. Each asymmetric division in the lineage is susceptible to the effects of CHMP2B^{Intron5}. Furthermore, we demonstrate that the effect of CHMP2B^{Intron5} on ES organ development is achieved through an increase in Notch signaling. The potency of CHMP2B^{Intron5}, however, is not equivalent for each division, suggesting that each binary cell fate decision in the lineage may exhibit a different threshold for Notch function to actuate appropriate cell fate specification.

Materials and Methods

Drosophila stocks and crosses

Flies were raised on standard medium (Genesee, #66–112) at 25°C or at 20°C for temperature sensitive crosses. The following transgenic elements were obtained from stocks at the Bloomington Stock Center and combined with other elements via standard Mendelian genetics to generate working stocks for crosses: *neur^{P72}-Gal4* (BL#80575), *pnr^{MD237}-Gal4* (BL#3037), *EQ-Gal4* (BL#43659), *tubGal80^{ts}* (BL#7018), *UAS-N^{intra}* (BL#52008), *NRE-GFP* (BL#30727, 30728). Other transgenic elements included *UAS-CHMP2B^{WT}* and *UAS-CHMP2B^{Intron5}* (Ahmad et al., 2009), *ase-Gal4* (a gift from E. Lai), and *Pax2^{B}-Gal4*, which was generated as described below. *N^{ts1}* (Shellenbarger & Mohler, 1975), *Dl^{RevF10}* (Haenlin, Kramatschek, & Campos-Ortega, 1990), and *Su(H)^{AR9}* (Schweisguth & Posakony, 1992) were used to reduce dosage of the respective genes and were gifts from E. Lai (*N^{ts1}*, *Dl^{RevF10}*) and J. Posakony (*Su(H)^{AR9}*). Fly stocks with the transgenic elements required for various crosses were generated by standard crossing and recombination. The initial crosses involved crossing the specific *Gal4* lines with either –

UAS-CHMP2B^{Intron5};tubGal80^{ts}/T(2;3)SM5;TM6B or

UAS-CHMP2B^{WT};tubGal80^{ts}/T(2;3)SM5;TM6B.

The following crosses was performed to reduce dosage of Notch pathway genes –

N^{ts1};neur-Gal4/TM6B × *UAS-CHMP2B^{Intron5};tubGal80^{ts}/T(2;3)SM5;TM6B*.

neur-GAL4, tubGAL80/TM6B × UAS-CHMP2B^{Intron5}/CyO; Dl^{RevF10}/MKRS

Su(H)^{AR9}; neur-GAL4/SM5TM6B × UAS-CHMP2B^{Intron5};tubGal80^{ts}/ T(2;3)SM5;TM6B

The following crosses were performed to assess Notch activity via the *NRE-GFP* reporter –

NRE-GFP;pnr-Gal4/T(2;3)SM5;TM6B x

UAS-CHMP2B^{Intron5};tubGal80^{ts}/T(2;3)SM5;TM6B and

pnr-Gal4, tubGal80^{ts}/TM6B × *UAS-N^{Intra};NRE-GFP/T(2;3)SM5;TM6B.*

For all experiments requiring temperature shift, white prepupae were selected and placed in petri dishes with a small damp sponge to provide moisture. The dishes were incubated at 20°C for the designated times and then placed in a 29°C incubator for the duration of the temperature shift.

Generation of *Pax2^{B}-Gal4* flies

A 3.1 kb enhancer was excised using BamHI from the pH-Stinger construct used to generate *Pax2^{B}-GFP* transgenic flies (Johnson, Harmon, Smiley, Still, & Kavaler, 2011). This insert was cloned into the pPTGAL4 BamHI site (Sharma, Cheung, Larsen, & Eberl, 2002). A successful construct was verified by restriction enzyme analysis and sequence analysis of the 5' and 3' ends. The construct was injected into fly embryos along with the pUChsΔ2–3 helper plasmid by standard techniques (Cripps & Bernstein, 2000) and the resulting progeny were crossed to *w^{1118}* flies. Several *w^{+}* progeny were isolated, the transgenes were mapped to specific chromosomes, and stocks were produced by balancing over either *CyO* or *TM6B* balancer chromosomes. The stock used contained a *Pax2^{B}-Gal4* transgene on chromosome III.

Imaging of adult flies and quantification of *Drosophila* microchaetes

Images of adult flies were taken using a Zeiss Discovery V12 stereomicroscope with a Zeiss AxioCam MRc5 at 200X magnification. For each image, frames covering the entire notum at focal planes 25 μm apart were taken and processed using the Zen2 software extended plane of focus function. For quantification, we designated a box region on the dorsal thorax bounded by the dorsocentral macrochaetes on the sides, the transverse suture near the wing on the top, and the scutal-scutellar suture on the bottom. Within this region, shafts were counted manually with the aid of Adobe Illustrator (Version 22.0.1).

Immunohistochemistry and imaging

White prepupae were aged for specified times and dissected. The tissue was fixed for 20 to 30 minutes in 4% paraformaldehyde in phosphate-buffered saline (PBS, Sigma) and washed extensively in PBS with 0.1% Triton X-100 (PBT). The tissue was stained with primary or secondary antibodies diluted in blocking solution (2% BSA in PBT) by incubating at room temperature for 3 hours or at 4°C overnight. Tissues were washed 6 times with PBT in between primary and secondary antibody incubations, and then mounted in Fluoro-Gel II with DAPI (Electron Microscopy Sciences, #17985–50). Primary antibodies used were rat anti-Elav (1:200, Developmental Studies Hybridoma Bank, 7E8A10), rabbit anti-DPax2 (1:10000, J. Kavaler) (Johnson et al., 2011), mouse anti-Cut (1:100, Developmental Studies Hybridoma Bank, 2B10), guinea pig anti-Senseless (a gift from H. Bellen) (Nolo, Abbott, & Bellen, 2000) and goat-anti-Suppressor of Hairless (1:200, Santa Cruz Biotechnology #sc-15813). Secondary antibodies were donkey anti-rabbit IgG-FITC (1:1000 Santa Cruz Biotechnology #sc-2090), donkey anti-goat IgG-TexasRed (1:1000 Santa Cruz Biotechnology #sc-2783), and donkey anti-rat IgG-DyLight 650 (1:1000 Thermo Scientific #SA5–10029).

Images were taken with a Zeiss Axioimager.A2 fluorescence microscope using EC Plan neofluar 10X, 20X, and 40X oil lenses and an Axiocam MRm camera. Images were processed using Zen2 software and Adobe Photoshop CS6, including gamma adjustments.

Results

Ectopic expression of *CHMP2B^{Intron5}* in the *Drosophila* notum leads to profound loss of ES organ shafts.

Previous work has shown that CHMP2B^{Intron5} expression in *Drosophila* can lead to neurodegeneration or abnormal neural development in the eye (Ahmad et al., 2009; Cheruiyot et al., 2014). To test the sensitivity with which CHMP2B^{Intron5} can affect critical signaling processes, we misexpressed it in the *Drosophila* notum using the Gal4/UAS system and examined its effect on ES organ development. Initially we used a panel of five *Gal4* lines – *pnr-Gal4*, *EQ-Gal4*, *neur^{P72}-Gal4*, *Pax2^{B}-Gal4*, and *ase-Gal4* – that are known to drive expression in the notum during larval and pupal development. Several of the lines also drive expression during embryonic development and caused embryonic or early larval lethality, suggesting a potent effect of ectopic CHMP2B^{Intron5} (but not CHMP2B^{WT}) on essential unidentified signaling pathways (data not shown). To constrain ectopic CHMP2B^{Intron5} expression to time points during adult ES organ development, we introduced a ubiquitously expressed temperature-sensitive allele of the Gal80 repressor (*tubGal80^{ts}*) into the crosses (McGuire, Le, Osborn, Matsumoto, & Davis, 2003). By incubating the crosses at a permissive temperature (20–22°C) until pupation and then shifting to the restrictive temperature (29°C), we were able to constrain CHMP2B^{Intron5} expression both spatially (via each *Gal4* line pattern) and temporally (via temperature) to primarily affect notum ES organ development. By selecting and incubating white prepupae at 29°C for 24 hours, we were able to induce CHMP2B^{Intron5} expression throughout the critical time during which all the notum microchaete cells arise and are specified. Nota from all *Gal4* × CHMP2B^{Intron5} crosses exhibited some degree of microchaete shaft loss, including *Gal4* lines that drive expression in broad domains across the notum (*EQ-Gal4* and *pnr-Gal4*) as well as *Gal4* lines that drive expression specifically in developing ES cells (*neur^{P72}-Gal4*, *Pax2^{B}-Gal4*, *ase-Gal4*) (Figure 2). All lines tested caused some defects in external bristle morphology (most notably loss of shafts or ES organs). *EQ-Gal4* and *pnr-Gal4* also created severe defects in the formation of the dorsal thorax most likely related to dorsal closure and/or thorax growth (Figure 2B,C). When compared to expression of CHMP2B^{WT} (Figure 2A,G), the strongest effect specific to ES organs was seen in *neur>CHMP2B^{Intron5}* flies, which created nota that were almost completely devoid of shafts (Figure 2D,H). The *neur^{P72}-Gal4* line was created by recombining a *Gal4* cassette into the *A101* (*neur-lacZ*) enhancer trap line (Bellaiche, Gho, Kaltschmidt, Brand, & Schweisguth, 2001) which expresses *lacZ* specifically in the pI cell as well as all the progeny cells throughout the cell division and specification phase of ES organ development (Usui & Kimura, 1993). For these reasons, we selected this driver for further experiments.

CHMP2B^{Intron5} affects cell fate decisions throughout the ES lineage.

To determine the shortest period during which CHMP2B^{Intron5} could exert its effect on ES organ development, we designed three different temperature shift regimens. Normally,

developing pupae are staged by selection as white prepupae followed by incubation at 25°C. The sequential cell divisions which generate the microchaete ES organ cells occur more or less synchronously at 25°C (Figure 1B, upper timeline). However, the temperature sensitivity of the *Gal80^{ts}* mutant is somewhat leaky at 25°C such that pupae raised at this temperature without shifting to 29°C show some shaft loss (data not shown). To avoid this confounding effect, we aged *wild-type* pupae (in this study, *w^{1118}*, as all the transgenic lines were established in the *w^{1118}* background) at 20°C for specific times, then dissected and stained them to establish a corresponding timeline for ES cell divisions at 20°C (Figure 1B, Supplementary Figure 1).

Subsequently, *neur>CHMP2B^{WT}* and *neur>CHMP2B^{Intron5}* pupae were shifted to the restrictive temperature after they had been aged at 20°C for 12 hours after puparium formation (APF) (prior to pI specification and neur-Gal4 activity), 20 hours APF (post pI specification but prior to pI division), and 28 hours APF (post pI division). The temperature shifts were allowed to proceed throughout the ES cell specification period (16 hours, 12 hours, and 8 hours, respectively) with each ending at a developmental stage that corresponded to approximately 24 hours APF at 25°C, a time when the ES cell divisions and fate specification have concluded. We note that there is a lag time between the onset of the restrictive temperature and the production of CHMP2B^{Intron5} protein, most likely around 2 hours. This lag time was determined by using *neur-Gal4* in the presence *Gal80^{ts}* to drive GFP expression. White prepupae were selected and aged for 20 hours at 20°C and then shifted to 29°C. Nota were assessed for GFP fluorescence every two hours. There is no observable GFP present in the aged pupae prior to temperature shift but GFP can be detected at a low level after two hours at 29°C and GFP signal increases with time (Supplementary Figure 2).

Nota from *neur>CHMP2B^{WT}* pupae that underwent temperature shift at any of the three time points showed no noticeable shaft loss (Figure 3D). Nota from *neur>CHMP2B^{Intron5}* pupae that were shifted to 29°C starting at 12 hours APF were similar to those that had undergone temperature shift from the beginning of pupation in that they also exhibited complete loss of shafts (Figure 3A,D; compare with Figure 2D). Nota from *neur>CHMP2B^{Intron5}* pupae that were shifted to 29°C starting at 20 hours APF showed strong, but not complete, shaft loss (Figure 3B,D). Nota from *neur>CHMP2B^{Intron5}* pupae that were shifted to 29°C starting at 28 hours APF showed little to no shaft loss. The severity of shaft loss caused by CHMP2B^{Intron5} differed significantly at each time point ($p = 1.45e-07$ for 12 hours versus 20 hours, $p = 1.00e-09$ for 12 hours versus 28 hours, and $p = 2.22e-10$ for 20 hours versus 28 hours by Welch's two sample t-test). These results show that restricting CHMP2B^{Intron5} expression to the time window of the establishment of the pI cell through all the ES cell divisions is capable of generating extensive loss of shafts (Figure 3C).

To ascertain if the cause of shaft loss is due to cell fate transformation, we dissected nota of *neur>CHMP2B^{Intron5}* pupae that had been shifted to 29°C starting at 20 hours APF (which is equivalent to the shaft loss shown in Figure 3B). By staining with antibodies that recognize the neuron (anti-Elav)(Robinow & White, 1991), socket cell (anti-Suppressor of Hairless (Su(H))(Gho, Lecourtois, Geraud, Posakony, & Schweisguth, 1996), and shaft and sheath cells (anti-DPax2; large nucleus of shaft, small nucleus of sheath) (Kavaler, Fu, Duan,

Noll, & Posakony, 1999), we are able to identify the four cell types in a differentiating ES organ. The normal composition of these four cell types is evident in control staining of *neur>CHMP2B^{WT}* nota (Figure 4A,C). In contrast, the overwhelming majority (>95%) of ES organs in *neur>CHMP2B^{Intron5}* nota show loss of the large DPax2^{+} nucleus in conjunction with a second Su(H)$^{+}$ nucleus (Figure 4B,D). This phenotype is consistent with a shaft-to-socket cell transformation. A small percentage of these affected ES organs also show the loss of the Elav^{+} nucleus in conjunction with a second small DPax2^{+} nucleus (Figure 4B, arrow, and Figure 4E), consistent with a neuron-to-sheath cell transformation. Also on rare occasions, an affected ES organ contained four Su(H)$^{+}$ socket cells (Figure 4B, arrowhead, and Figure 4F), consistent with a pIIB to pIIA cell transformation followed by a shaft to socket cell transformation. Therefore, the loss of shafts seen in *neur>CHMP2B^{Intron5}* nota is the result of shaft to socket cell transformations. Additionally, expression of CHMP2B^{Intron5} in the ES organ lineage can cause other cell fate transformations ES organ cell lineage (neuron to sheath cell and pIIB to pIIA cell transformations).

Reduction in Notch gene dosage partially rescues *neur>CHMP2B^{Intron5}* bristle shaft loss phenotype.

The cell fate transformations seen in *neur>CHMP2B^{Intron5}* flies correspond to transformations seen when Notch activity is increased during cell fate specification (Bang & Posakony, 1992; Guo, Jan, & Jan, 1996). ES organs exhibiting neuron, sheath cell, and two socket cells hint at an increased Notch signal that overcomes only the shaft-socket specification. ES organs exhibiting two sheath cells and two socket cells suggest both neuron-sheath and shaft-socket specifications have been altered. ES organs exhibiting four socket cells suggest the pIIA-pIIB and shaft-socket specifications have been altered.

If CHMP2B^{Intron5} expression is indeed leading to an upregulation of Notch activity and this increase is responsible for the cell fate changes we observe, then reduction of the dosage of *Notch* might suppress the effect. Therefore, we crossed females bearing *neur-Gal4* and *N^{ts1}* (a temperature-sensitive allele of *Notch* that is functional at the permissive temperature but nonfunctional at the restrictive temperature used in our regimen) to males bearing *UAS-CHMP2B^{Intron5} and tubGal80^{ts}*. Female progeny arising from the cross are *N^{+}/N^{ts1}* and would therefore have a reduced dosage of *Notch* upon temperature shift. Compared to *neur>CHMP2B^{Intron5}* flies with normal *Notch* dosage, *neur>CHMP2B^{Intron5}* flies with reduced *Notch* dosage showed an increase in the number of shafts evident on the notum ($p = 1.73e-05$), albeit not a complete rescue (Figure 5B, C, F). In contrast, reduced dosage of two other genes in the Notch pathway, *Delta* (*Dl*) and *Su(H)*, had no effect on the *neur>CHMP2B^{Intron5}* shaft loss phenotype (Figure 5D–F).

Expression of *CHMP2B^{Intron5}* in the notum corresponds to increased Notch activity.

To assess whether expression of *CHMP2B^{Intron5}* leads to an upregulation of Notch activity, we utilized a Notch-responsive reporter line (*NRE-GFP*) (Stempfle, Kanwar, Loewer, Fortini, & Merdes, 2010). This reporter is capable of identifying cells undergoing significant Notch activation, such as cells at the wing margin in third instar larval wing imaginal discs (Zacharioudaki & Bray, 2014). To test the ability of the *NRE-GFP* reporter in detecting

upregulated Notch signaling in the notum, we misexpressed the constitutively active Notch intracellular domain (NICD) using the *pnr-Gal4* driver. The advantage of the *pnr-Gal4* line for this experiment is that it drives expression in a broad medial region in the developing notum, thereby allowing the lateral portions of the notum to serve as an internal negative control. Although *pnr>NICD* by itself is embryonic lethal, we again included $Gal80^{ts}$ to control the timing of expression. Expression of NICD in the notum during the time when ES organs develop led to clear *NRE-GFP* reporter expression only in expected medial regions (Figure 6A,A'). In comparison to *pnr>NICD* nota, $pnr>CHMP2B^{Intron5}$ nota showed GFP expression in a similar pattern, albeit expression was weaker, more variegated, and absent from the scutellar region (Figure 6B,B'). We observed strong reporter expression along the line of the dorsocentral macrochaetes and weaker expression in occasional clusters of cells. In the domain outside of *pnr-Gal4* expression, we observed GFP in some single cells (and occasional doublets). The single cells are socket cells which are beginning to differentiate and express high levels of Su(H) protein (Gho et al., 1996). To make sure that the *NRE-GFP* reporter expression is caused by $CHMP2B^{Intron5}$ expression and not simply an artifact of the heat shock regimen, we repeated the experiment in the absence of $UAS\text{-}CHMP2B^{Intron5}$. In this case, GFP is still observable in socket cells but both the strong and weak clustered expression of GFP in the *pnr-Gal4* expressing domain is absent (Figure 6C,C'). These results suggest that expression of $CHMP2B^{Intron5}$ broadly in the notum is capable of inducing high levels of Notch activity.

Discussion

Human $CHMP2B^{Intron5}$, the predominant protein variant of CHMP2B associated with FTD in a Danish lineage, acts as a gain-of-function form that interferes with normal endosomal-lysosomal trafficking (Skibinski et al., 2005). Although the mechanism by which it causes FTD is unknown, several lines of evidence point to its ability to disrupt cell signaling pathways by blocking the cell surface receptor turnover. Transfection of fibroblasts from FTD patients with $CHMP2B^{Intron5}$ leads to decreased endosome-lysosome fusion and inhibits degradation of the EGF receptor (Urwin et al., 2010). Misexpression of $CHMP2B^{Intron5}$ in *Drosophila* photoreceptors causes upregulated Toll receptor signaling and neurodegeneration (Ahmad et al., 2009) while misexpression in the eye earlier during development causes abnormal accumulation of Notch receptor and massive eye deformities (Cheruiyot et al., 2014). When introduced into *Drosophila* neurons, $CHMP2B^{Intron5}$ is associated with enhanced levels of TGF-β and JNK signaling and increased synaptic growth (West, Lu, Marie, Gao, & Sweeney, 2015). In this study, we have assessed the ability of $CHMP2B^{Intron5}$ to impede peripheral nervous system development in a new setting, the ES organs (or bristles) on the dorsal thorax of the fly. Because each bristle arises from a single cell which undergoes a series of sequential divisions to produce four distinct cell types, the results of cell fate decisions at specific time points can be monitored easily and with precision. Furthermore, using available *Gal4* lines in combination with a temperature sensitive allele of *Gal80*, we can restrict expression of $CHMP2B^{Intron5}$ specifically to ES cells during cell fate specification. We find that ectopic expression of $CHMP2B^{Intron5}$ (but not $CHMP2B^{WT}$) severely disrupts ES organ development, leading to a number of cell fate transformations. Each type of cell fate transformation observed is reminiscent of phenotypes

historically associated with gain-of-function Notch signaling. In addition, the effects of CHMP2B^{Intron5} can be suppressed by reducing Notch gene levels. Finally, we observe that a reporter for Notch activation (*NRE-GFP*) shows increased activity when CHMP2B^{Intron5} is expressed. All together, these data indicate that CHMP2B^{Intron5} can cause dramatic effects in a short developmental time window by disrupting the normal function of Notch, leading to a heightened level of signaling that generates inappropriate cell fate changes. While ancillary signaling pathways have not been ruled out, Notch is the predominant signaling pathway acting during ES organ development. Our ability to control CHMP2B^{Intron5} expression in concert with the fact that Notch signaling is used iteratively during ES organ development has allowed us to assess the effects of CHMP2B^{Intron5} expression at each cell fate decision.

The effects of expressing CHMP2B^{Intron5} in the developing nervous system were so profound that all but one of the *Gal4* drivers we tested led to embryonic/early larval death. When we restricted expression of CHMP2B^{Intron5} to the early pupal stage, all lines were capable of disrupting ES organ development in such a manner that most shafts were no longer evident. Loss of shafts can result from a few different events: 1) loss of the pI (SOP) cell, 2) transformation of the shaft cell into a socket cell, 3) transformation of the pIIA cell into a pIIB cell, or 4) failure of a specified shaft cell to differentiate properly. The first two events occur when there is excess Notch signaling, which causes the transformation of the missing cells by inhibiting their normal cell fate specification. The third possibility would suggest an opposite mechanism whereby Notch signaling is lessened thereby converting the normally Notch-sensitive pIIA cell into a second pIIB which would then generate an extra neuron and sheath cell at the expense of the external cell types. Two pieces of evidence suggest that the primary effect of CHMP2B^{Intron5} misexpression in the ES organ lineage is to cause a transformation of the shaft cell into a second socket cell. First, the external appearance of the notum is not strictly smooth as one might expect for either loss of pI or for pIIA to pIIB transformation, but instead shows small protuberances in an orderly array indicating the presence of one or more sockets at each bristle position (Figure 2). Second, immunohistochemistry on notum tissue shows the vast majority of bristle positions contain the normal complement of four bristle cells of which two express the socket cell marker Su(H) (Figure 4).

The immunohistochemical examination showed that most altered positions contained the normal internal cells (neuron and sheath) along with two socket cells and no shaft cells, as would be expected if only the socket/shaft decision were affected. However, there were rare instances (fewer than five per notum) of double sheath cell/double socket cell positions, indicating both neuron to sheath cell and shaft cell to socket cell transformations. There were also rare instances (again, fewer than five per notum) of four socket positions, indicating cell fate transformations at both the pIIA/pIIB decision and the socket/shaft decision. It is unclear why the socket/shaft decision was so easily perturbed while the other cell fate decisions were more resistant to treatment. It is possible that the socket/shaft decision is more sensitive to changes in Notch activity. Alternatively, the expression of CHMP2B^{Intron5} is uneven in the different cells of the lineage and has greater expression in the shaft/socket lineage, although expression of GFP by the same driver seems relatively uniform among the cells (Supplementary Figure 2).

Each cell fate change is consistent with increased Notch activity at each cell specification decision point. This hypothesis is supported by the observation that downregulating the dosage of Notch is capable of suppressing the shaft loss phenotype as lower Notch levels restore the signaling balance during lineage cell specification. We note reduced copy number of other genes in the Notch pathway (*Delta* and *Su(H)*) did not have an observable restorative effect on shaft number (Figure 5). Furthermore, when we assessed the intensity of Notch signaling in response to CHMP2B^{Intron5} (visualized using a Notch-responsive reporter), it was elevated across the notum in the wake of broad, *pnr-Gal4* driven expression of CHMP2B^{Intron5} (Figure 6B,B'). The pattern of Notch activity detected was uneven across the area of expression, although it roughly resembled the pattern seen when an activated form of Notch was similarly expressed (Figure 6A,A'). In contrast to the effect of ectopic expression of NICD, CHMP2B^{Intron5} seems to be a less effective activator of the NRE-GFP except along the midline and anterior posterior columns surrounding the dorsocentral macrochaetes, where it is quite strong. Interestingly, whereas NICD demonstrates activity in the scutellar region, where no microchaetes form in wild-type flies, CHMP2B^{Intron5} shows no ability to activate the pathway in this region. This result suggests that although the scutellar region is competent to receive an activated Notch signal, it is insensitive to the actions of CHMP2B^{Intron5} perhaps because it is normally devoid of microchaetes.

The ability of CHMP2B^{Intron5} to increase levels of Notch activity has been demonstrated previously in the *Drosophila* eye. Misexpression of CHMP2B^{Intron5} in the eye has been shown to cause an accumulation of Notch in enlarged endosomes, leading to an increase in Notch signaling and overproliferation of eye tissue (Cheruiyot et al., 2014). Misexpression in the ES organ lineage does not appear to lead to overproliferation (all bristle positions still have 4 cells) but does act in a manner consistent with a gain of Notch function. Instead, the consequences of introducing CHMP2B^{Intron5} in the ES organ lineage involve the transformation of cell fate. Receptor endocytosis is often considered a mechanism by which signaling pathways can be downregulated. Therefore, disruption of receptor endocytosis leads to upregulation of receptor signaling. In this study, CHMP2B^{Intron5}–mediated disruption of the endosomal-lysosomal pathway results in upregulation of Notch signaling which may occur through two potential mechanisms – 1) retention of Notch in the plasma membrane via blockage of endosome entry and/or, 2) retention of Notch in endosomes, leading to decreased receptor degradation. There is a body of evidence that trafficking of Notch through endosomal compartments is associated with Notch signaling activity (Fortini, 2009). Another ESCRT-III component, shrub, has been shown to attenuate Notch signaling by promoting degradation of the receptor. Loss of shrub leads to enhanced Notch activity in late endosomes (Hori, Sen, Kirchhausen, & Artavanis-Tsakonas, 2011). In addition, loss of the gene lethal (2) giant discs, a regulator of endosomal trafficking, leads to accumulation of Notch in enlarged endosomes and activation of the receptor in the lysosome (Schneider, Troost, Grawe, Martinez-Arias, & Klein, 2013). Related observations have been made with regard to Notch signaling in the ES cell lineage. In the pIIA cell but not the pIIB cell, Notch is segregated to endosomes containing the protein Sara and is cleaved in these endosomes to generate the active NICD component (Coumailleau, Furthauer, Knoblich, & Gonzalez-Gaitan, 2009; Loubery et al., 2014). Given the inability of reduced Dl dosage to rescue the CHMP2B^{Intron5} phenotype, we may be observing a noncanonical, ligand-independent

activation of Notch from interior cell compartments. CHMP2B^{Intron5} may act to increase the levels of endosomal Notch available for such activation.

It has been observed that blocking endosome entry prevents the accumulation of NICD (Fortini & Bilder, 2009; Vaccari, Lu, Kanwar, Fortini, & Bilder, 2008). In contrast, in the pIIB cell, the asymmetrically distributed protein Numb promotes movement of Notch to the late endosome compartment and depresses receptor recycling to the membrane (Johnson, Zitserman, & Roegiers, 2016; Kandachar & Roegiers, 2012). CHMP2B^{Intron5} may therefore act by disrupting flow of Notch to the late endosome compartment, thereby raising the levels of Notch available on the cell surface for canonical signaling in the Notch-resistant cells in the lineage (pIIB, shaft cell, neuron). Our previous work demonstrated such an effect in the eye (Cheruiyot et al., 2014). Further work is required to tease apart these possibilities. In either case, the disruption of general cellular membrane trafficking machinery via CHMP2B^{Intron5} is capable of inducing potent phenotypes associated with elevated Notch signaling.

Supplementary Material

Refer to Web version on PubMed Central for supplementary material.

Acknowledgments

We thank Eric Lai, Hugo Bellen, the Bloomington Stock Center, and the Developmental Studies Hybridoma Bank for fly stocks and antibodies. We thank Mike Zheng for reviewing and providing comments on the manuscript. S. Tariq Ahmad is supported by an Institutional Development Award (IDeA) from the National Institute of General Medical Sciences of the National Institutes of Health under grant number P20GM103423 and science division grant from Colby College.

References

Ahmad ST, Sweeney ST, Lee JA, Sweeney NT, & Gao FB (2009). Genetic screen identifies serpin5 as a regulator of the toll pathway and CHMP2B toxicity associated with frontotemporal dementia. Proc Natl Acad Sci U S A, 106(29), 12168–12173. doi:10.1073/pnas.0903134106 [PubMed: 19581577]

Bang AG, & Posakony JW (1992). The Drosophila gene Hairless encodes a novel basic protein that controls alternative cell fates in adult sensory organ development. Genes Dev, 6(9), 1752–1769. Retrieved from http://www.ncbi.nlm.nih.gov/entrez/query.fcgi?cmd=Retrieve&db=PubMed&dopt=Citation&list_uids=1516831 [PubMed: 1516831]

Bellaiche Y, Gho M, Kaltschmidt JA, Brand AH, & Schweisguth F (2001). Frizzled regulates localization of cell-fate determinants and mitotic spindle rotation during asymmetric cell division. Nat Cell Biol, 3(1), 50–57. doi:10.1038/35050558 [PubMed: 11146626]

Belly A, Bodon G, Blot B, Bouron A, Sadoul R, & Goldberg Y (2010). CHMP2B mutants linked to frontotemporal dementia impair maturation of dendritic spines. J Cell Sci, 123(Pt 17), 2943–2954. doi:10.1242/jcs.068817 [PubMed: 20699355]

Chassefeyre R, Martinez-Hernandez J, Bertaso F, Bouquier N, Blot B, Laporte M, … Goldberg Y(2015). Regulation of postsynaptic function by the dementia-related ESCRT-III subunit CHMP2B. J Neurosci, 35(7), 3155–3173. doi:10.1523/JNEUROSCI.0586-14.2015 [PubMed: 25698751]

Cheruiyot A, Lee JA, Gao FB, & Ahmad ST (2014). Expression of mutant CHMP2B, an ESCRT-III component involved in frontotemporal dementia, causes eye deformities due to Notch misregulation in Drosophila. FASEB J, 28(2), 667–675. doi:10.1096/fj.13-234138 [PubMed: 24158394]

Coumailleau F, Furthauer M, Knoblich JA, & Gonzalez-Gaitan M (2009). Directional Delta and Notch trafficking in Sara endosomes during asymmetric cell division. Nature, 458(7241), 1051–1055. doi:10.1038/nature07854 [PubMed: 19295516]

Cripps RM, & Bernstein SI (2000). Generation of transgenic Drosophila melanogaster by P element-mediated germline transformation In Norton PA & Steel LF (Eds.), Gene Transfer Methods (pp. 93–125). Natick, MA: Eaton Publishing.

Fortini ME (2009). Notch signaling: the core pathway and its posttranslational regulation. Dev Cell, 16(5), 633–647. Retrieved from http://www.ncbi.nlm.nih.gov/entrez/query.fcgi?cmd=Retrieve&db=PubMed&dopt=Citation&list_uids=19460341 [PubMed: 19460341]

Fortini ME, & Bilder D (2009). Endocytic regulation of Notch signaling. Curr Opin Genet Dev, 19(4), 323–328. doi:10.1016/j.gde.2009.04.005 [PubMed: 19447603]

Ghazi-Noori S, Froud KE, Mizielinska S, Powell C, Smidak M, Fernandez de Marco M, … Isaacs AM (2012). Progressive neuronal inclusion formation and axonal degeneration in CHMP2B mutant transgenic mice. Brain, 135(Pt 3), 819–832. doi:10.1093/brain/aws006 [PubMed: 22366797]

Gho M, Lecourtois M, Geraud G, Posakony JW, & Schweisguth F (1996). Subcellular localization of Suppressor of Hairless in Drosophila sense organ cells during Notch signalling. Development, 122(6), 1673–1682. Retrieved from http://www.ncbi.nlm.nih.gov/pubmed/8674407 [PubMed: 8674407]

Guo M, Jan LY, & Jan YN (1996). Control of daughter cell fates during asymmetric division: interaction of Numb and Notch. Neuron, 17(1), 27–41. Retrieved from http://www.ncbi.nlm.nih.gov/pubmed/8755476 [PubMed: 8755476]

Haenlin M, Kramatschek B, & Campos-Ortega JA (1990). The pattern of transcription of the neurogenic gene Delta of Drosophila melanogaster. Development, 110(3), 905–914. Retrieved from http://www.ncbi.nlm.nih.gov/pubmed/2128477 [PubMed: 2128477]

Hartenstein V, & Posakony JW (1990). A dual function of the Notch gene in Drosophila sensillum development. Dev Biol, 142(1), 13–30. Retrieved from http://www.ncbi.nlm.nih.gov/pubmed/2227090 [PubMed: 2227090]

Hori K, Sen A, Kirchhausen T, & Artavanis-Tsakonas S (2011). Synergy between the ESCRT-III complex and Deltex defines a ligand-independent Notch signal. J Cell Biol, 195(6), 1005–1015. doi:10.1083/jcb.201104146 [PubMed: 22162134]

Johnson SA, Harmon KJ, Smiley SG, Still FM, & Kavaler J (2011). Discrete regulatory regions control early and late expression of D-Pax2 during external sensory organ development. Dev Dyn, 240(7), 1769–1778. doi:10.1002/dvdy.22672 [PubMed: 21644243]

Johnson SA, Zitserman D, & Roegiers F (2016). Numb regulates the balance between Notch recycling and late-endosome targeting in Drosophila neural progenitor cells. Mol Biol Cell, 27(18), 2857–2866. doi:10.1091/mbc.E15-11-0751 [PubMed: 27466320]

Kandachar V, & Roegiers F (2012). Endocytosis and control of Notch signaling. Curr Opin Cell Biol, 24(4), 534–540. doi:10.1016/j.ceb.2012.06.006 [PubMed: 22818956]

Kavaler J, Fu W, Duan H, Noll M, & Posakony JW (1999). An essential role for the Drosophila Pax2 homolog in the differentiation of adult sensory organs. Development, 126(10), 2261–2272. Retrieved from http://www.ncbi.nlm.nih.gov/entrez/query.fcgi?cmd=Retrieve&db=PubMed&dopt=Citation&list_uids=10207150 [PubMed: 10207150]

Lai EC, & Orgogozo V (2004). A hidden program in Drosophila peripheral neurogenesis revealed: fundamental principles underlying sensory organ diversity. Dev Biol, 269(1), 1–17. Retrieved from http://www.ncbi.nlm.nih.gov/entrez/query.fcgi?cmd=Retrieve&db=PubMed&dopt=Citation&list_uids=15081353 [PubMed: 15081353]

Lee JA, Beigneux A, Ahmad ST, Young SG, & Gao FB (2007). ESCRT-III dysfunction causes autophagosome accumulation and neurodegeneration. Curr Biol, 17(18), 1561–1567. doi:10.1016/j.cub.2007.07.029 [PubMed: 17683935]

Loubery S, Seum C, Moraleda A, Daeden A, Furthauer M, & Gonzalez-Gaitan M (2014). Uninflatable and Notch control the targeting of Sara endosomes during asymmetric division. Curr Biol, 24(18), 2142–2148. doi:10.1016/j.cub.2014.07.054 [PubMed: 25155514]

McGuire SE, Le PT, Osborn AJ, Matsumoto K, & Davis RL (2003). Spatiotemporal rescue of memory dysfunction in Drosophila. Science, 302(5651), 1765–1768. doi:10.1126/science.1089035 [PubMed: 14657498]

Nolo R, Abbott LA, & Bellen HJ (2000). Senseless, a Zn finger transcription factor, is necessary and sufficient for sensory organ development in Drosophila. Cell, 102(3), 349–362. Retrieved from

http://www.ncbi.nlm.nih.gov/entrez/query.fcgi?cmd=Retrieve&db=PubMed&dopt=Citation&list_uids=10975525 [PubMed: 10975525]

Parks AL, & Muskavitch MA (1993). Delta function is required for bristle organ determination and morphogenesis in Drosophila. Dev Biol, 157(2), 484–496. doi:10.1006/dbio.1993.1151 [PubMed: 8500655]

Rhyu MS, Jan LY, & Jan YN (1994). Asymmetric distribution of numb protein during division of the sensory organ precursor cell confers distinct fates to daughter cells. Cell, 76(3), 477–491. Retrieved from http://www.ncbi.nlm.nih.gov/pubmed/8313469 [PubMed: 8313469]

Robinow S, & White K (1991). Characterization and spatial distribution of the ELAV protein during Drosophila melanogaster development. J Neurobiol, 22(5), 443–461. doi:10.1002/neu.480220503 [PubMed: 1716300]

Schneider M, Troost T, Grawe F, Martinez-Arias A, & Klein T (2013). Activation of Notch in lgd mutant cells requires the fusion of late endosomes with the lysosome. J Cell Sci, 126(Pt 2), 645–656. doi:10.1242/jcs.116590 [PubMed: 23178945]

Schweisguth F, & Posakony JW (1992). Suppressor of Hairless, the Drosophila homolog of the mouse recombination signal-binding protein gene, controls sensory organ cell fates. Cell, 69(7), 1199–1212. Retrieved from http://www.ncbi.nlm.nih.gov/entrez/query.fcgi?cmd=Retrieve&db=PubMed&dopt=Citation&list_uids=1617730 [PubMed: 1617730]

Schweisguth F, & Posakony JW (1994). Antagonistic activities of Suppressor of Hairless and Hairless control alternative cell fates in the Drosophila adult epidermis. Development, 120(6), 1433–1441. Retrieved from http://www.ncbi.nlm.nih.gov/pubmed/8050354 [PubMed: 8050354]

Scott CC, Vacca F, & Gruenberg J (2014). Endosome maturation, transport and functions. Semin Cell Dev Biol, 31, 2–10. doi:10.1016/j.semcdb.2014.03.034 [PubMed: 24709024]

Sharma Y, Cheung U, Larsen EW, & Eberl DF (2002). PPTGAL, a convenient Gal4 P-element vector for testing expression of enhancer fragments in drosophila. Genesis, 34(1–2), 115–118. doi:10.1002/gene.10127 [PubMed: 12324963]

Shellenbarger DL, & Mohler JD (1975). Temperature-sensitive mutations of the notch locus in Drosophila melanogaster. Genetics, 81(1), 143–162. Retrieved from http://www.ncbi.nlm.nih.gov/pubmed/812766 [PubMed: 812766]

Singhania A, & Grueber WB (2014). Development of the embryonic and larval peripheral nervous system of Drosophila. Wiley Interdiscip Rev Dev Biol, 3(3), 193–210. doi:10.1002/wdev.135 [PubMed: 24896657]

Skibinski G, Parkinson NJ, Brown JM, Chakrabarti L, Lloyd SL, Hummerich H, … Collinge J(2005). Mutations in the endosomal ESCRTIII-complex subunit CHMP2B in frontotemporal dementia. Nat Genet, 37(8), 806–808. doi:10.1038/ng1609 [PubMed: 16041373]

Stempfle D, Kanwar R, Loewer A, Fortini ME, & Merdes G (2010). In vivo reconstitution of gamma-secretase in Drosophila results in substrate specificity. Mol Cell Biol, 30(13), 3165–3175. doi:10.1128/MCB.00030-10 [PubMed: 20421416]

Stuffers S, Brech A, & Stenmark H (2009). ESCRT proteins in physiology and disease. Exp Cell Res, 315(9), 1619–1626. doi:10.1016/j.yexcr.2008.10.013 [PubMed: 19013455]

Urwin H, Authier A, Nielsen JE, Metcalf D, Powell C, Froud K, … Isaacs AM(2010). Disruption of endocytic trafficking in frontotemporal dementia with CHMP2B mutations. Hum Mol Genet, 19(11), 2228–2238. doi:10.1093/hmg/ddq100 [PubMed: 20223751]

Usui K, & Kimura KI (1993). Sequential emergence of the evenly spaced microchaetes on the notum of Drosophila. Roux Arch Dev Biol, 203(3), 151–158. doi:10.1007/BF00365054 [PubMed: 28305732]

Vaccari T, Lu H, Kanwar R, Fortini ME, & Bilder D (2008). Endosomal entry regulates Notch receptor activation in Drosophila melanogaster. J Cell Biol, 180(4), 755–762. doi:10.1083/jcb.200708127 [PubMed: 18299346]

van der Zee J, Urwin H, Engelborghs S, Bruyland M, Vandenberghe R, Dermaut B, … Van Broeckhoven C (2008). CHMP2B C-truncating mutations in frontotemporal lobar degeneration are associated with an aberrant endosomal phenotype in vitro. Hum Mol Genet, 17(2), 313–322. doi:10.1093/hmg/ddm309 [PubMed: 17956895]

Vernay A, Therreau L, Blot B, Risson V, Dirrig-Grosch S, Waegaert R, … Rene F (2016). A transgenic mouse expressing CHMP2Bintron5 mutant in neurons develops histological and behavioural features of amyotrophic lateral sclerosis and frontotemporal dementia. Hum Mol Genet, 25(15), 3341–3360. doi:10.1093/hmg/ddw182 [PubMed: 27329763]

West RJ, Lu Y, Marie B, Gao FB, & Sweeney ST (2015). Rab8, POSH, and TAK1 regulate synaptic growth in a Drosophila model of frontotemporal dementia. J Cell Biol, 208(7), 931–947. doi:10.1083/jcb.201404066 [PubMed: 25800055]

Zacharioudaki E, & Bray SJ (2014). Tools and methods for studying Notch signaling in Drosophila melanogaster. Methods, 68(1), 173–182. doi:10.1016/j.ymeth.2014.03.029 [PubMed: 24704358]

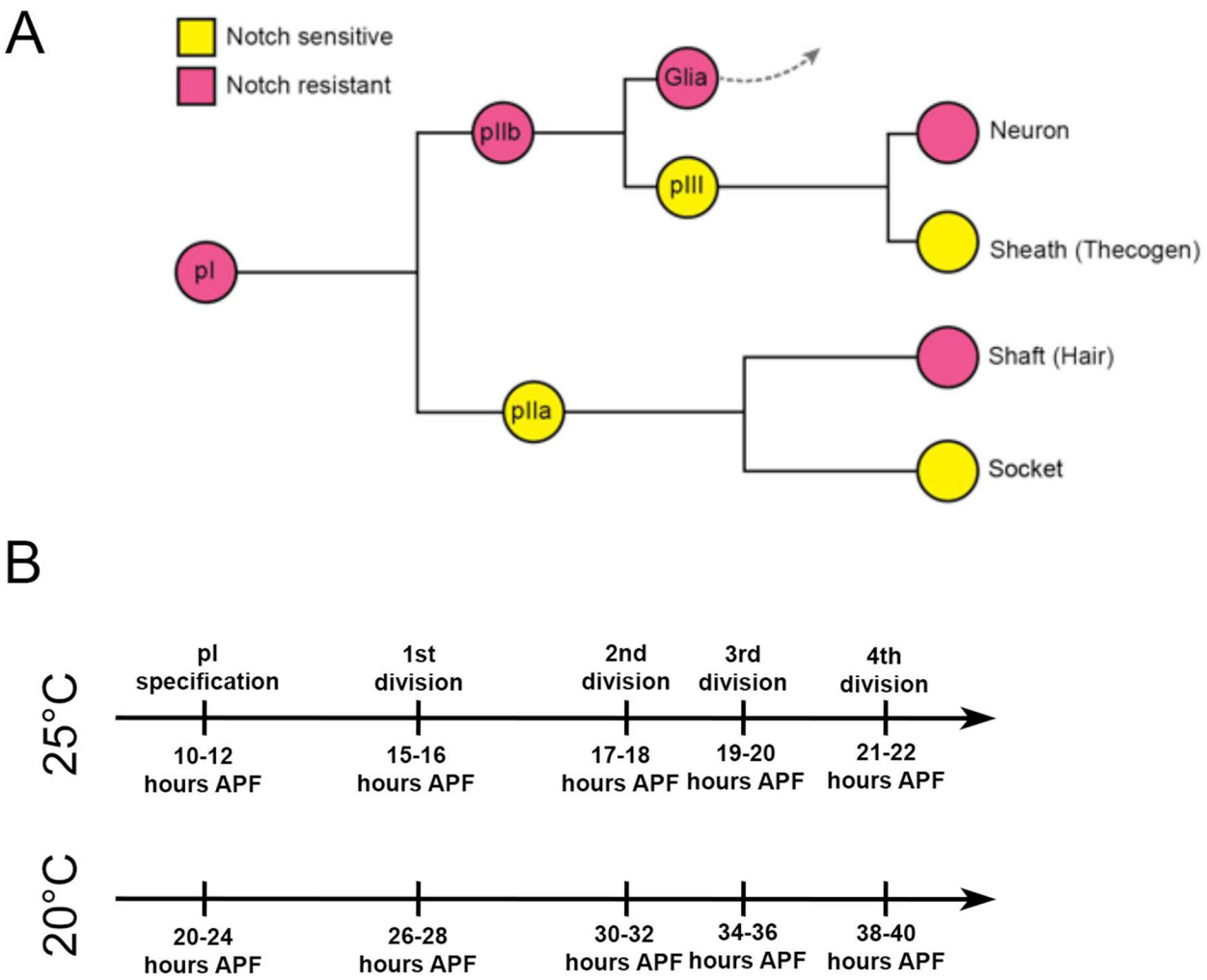

Figure 1.

A. Diagram of ES organ lineage divisions and cell fate specification. At each division, the fate of the resulting daughter cells is determined by whether they are resistant (marked in red) or sensitive (marked in yellow) to Notch signaling. The glial cell resulting from the division of pIIB migrates away from the other cells and undergoes apoptosis (curved arrow). B. Time course of ES organ cell divisions at 25°C (top) and 20°C (bottom). Times are marked as hours after puparium formation (APF).

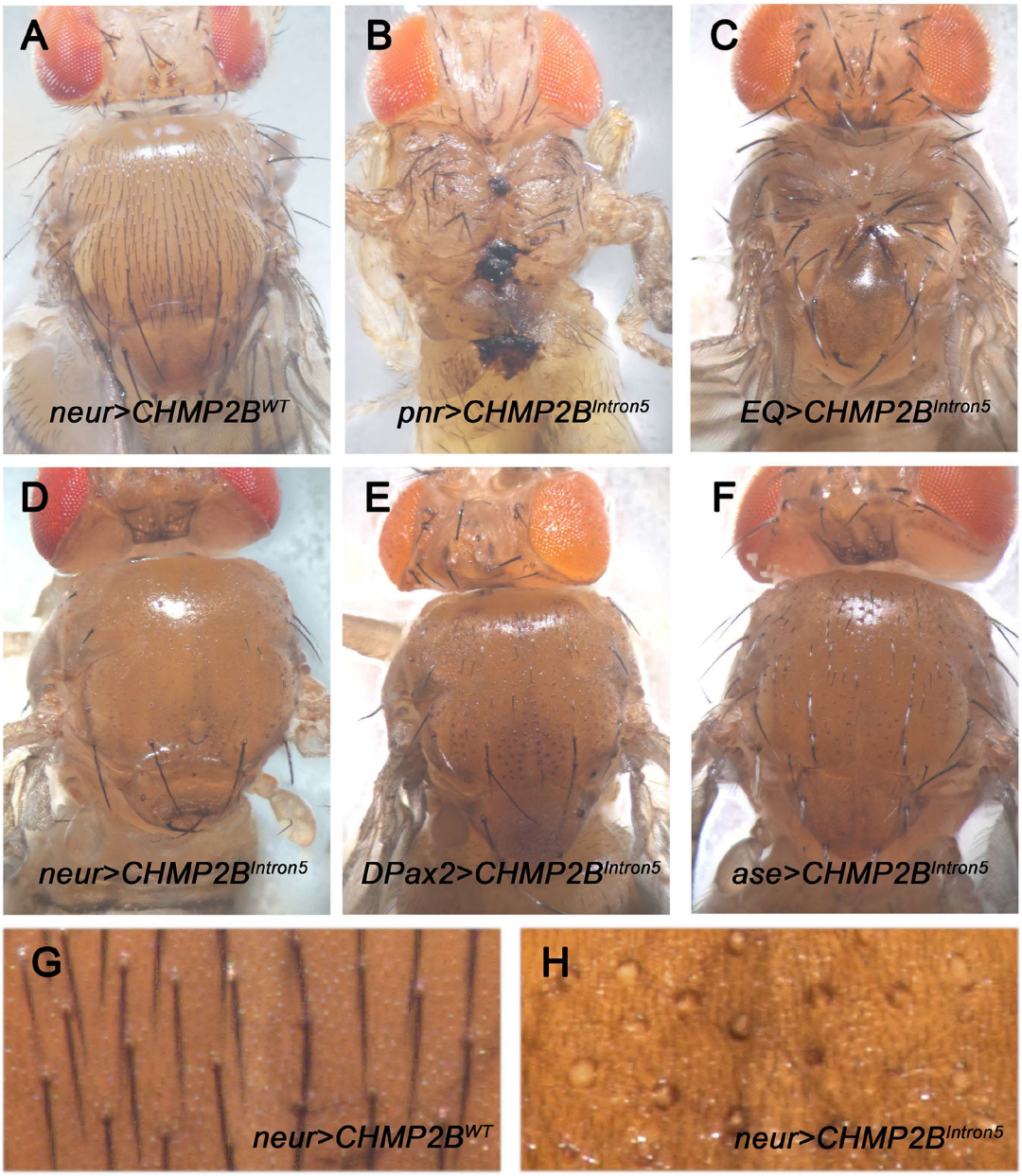

Figure 2.

Expression of CHMP2B^{Intron5} via a panel of *Gal4* lines causes defects in ES organ development. Images of dorsal thoraces of flies in which CHMP2B^{WT} (A, G) or CHMP2B^{Intron5} (B-F, H) were expressed using different *Gal4* drivers: *neur^{P72}-Gal4* (A, D, G and H), *pnr-Gal4* (B), *EQ-Gal4* (C), *Pax2^{B}-Gal4* (E), *ase-Gal4* (F). Panels G and H show close-ups of bristles from *neur>CHMP2B^{WT}* and *neur>CHMP2B^{Intron5}* dorsal thoraces, respectively.

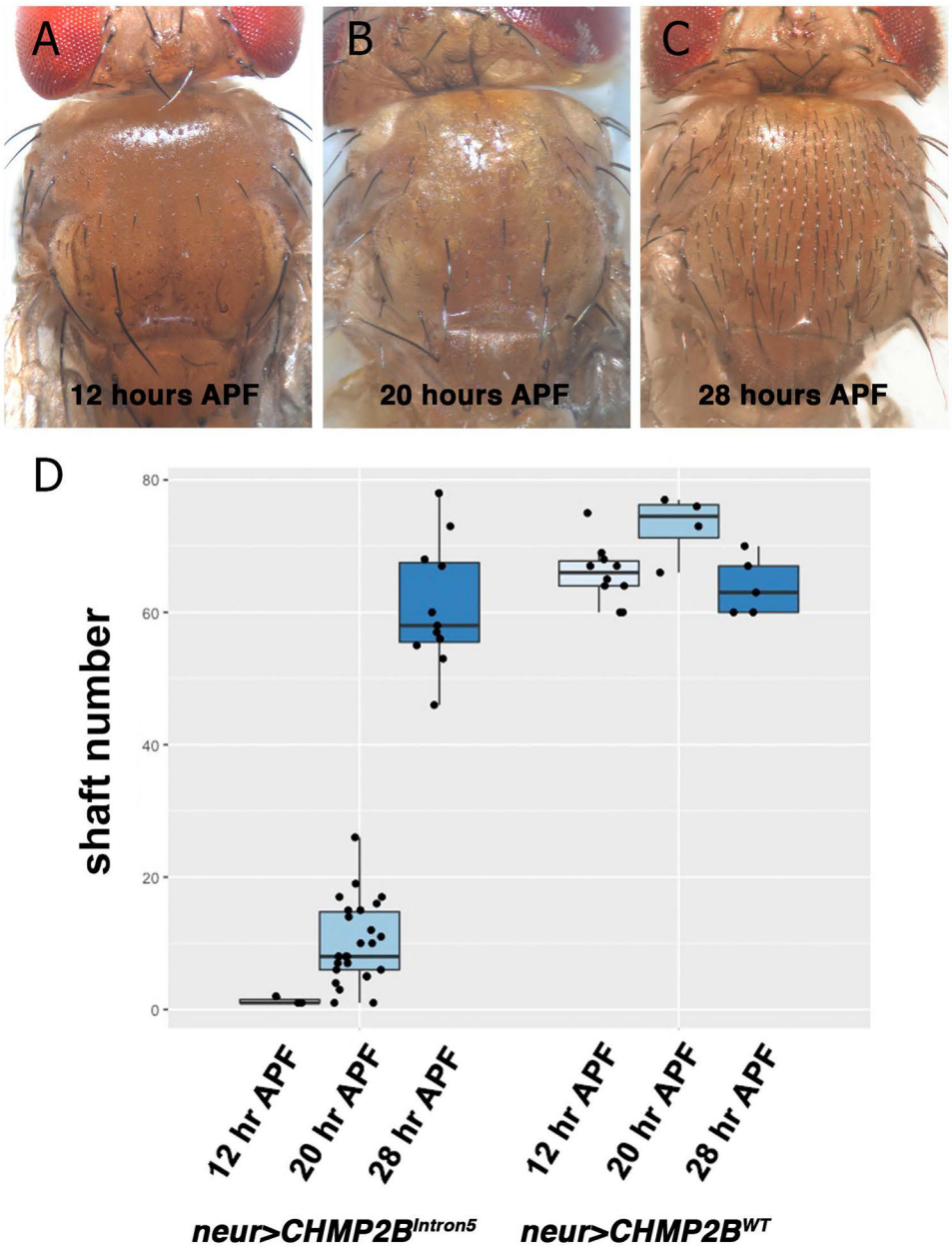

Figure 3.

Effect of timing of CHMP2B^{Intron5} expression driven by *neur^{P72}-Gal4* on shaft loss. Images of dorsal thoraces of flies in which CHMP2B^{Intron5} was expressed at 12 hours APF (A), 20 hours APF (B), 28 hours APF (C). D. Boxplot depicting quantification of shafts on the central region of the thorax. Lower and upper boundaries of the box mark the 25th and 75th percentile with the black line marking the median. The whiskers delineate the complete range of values.

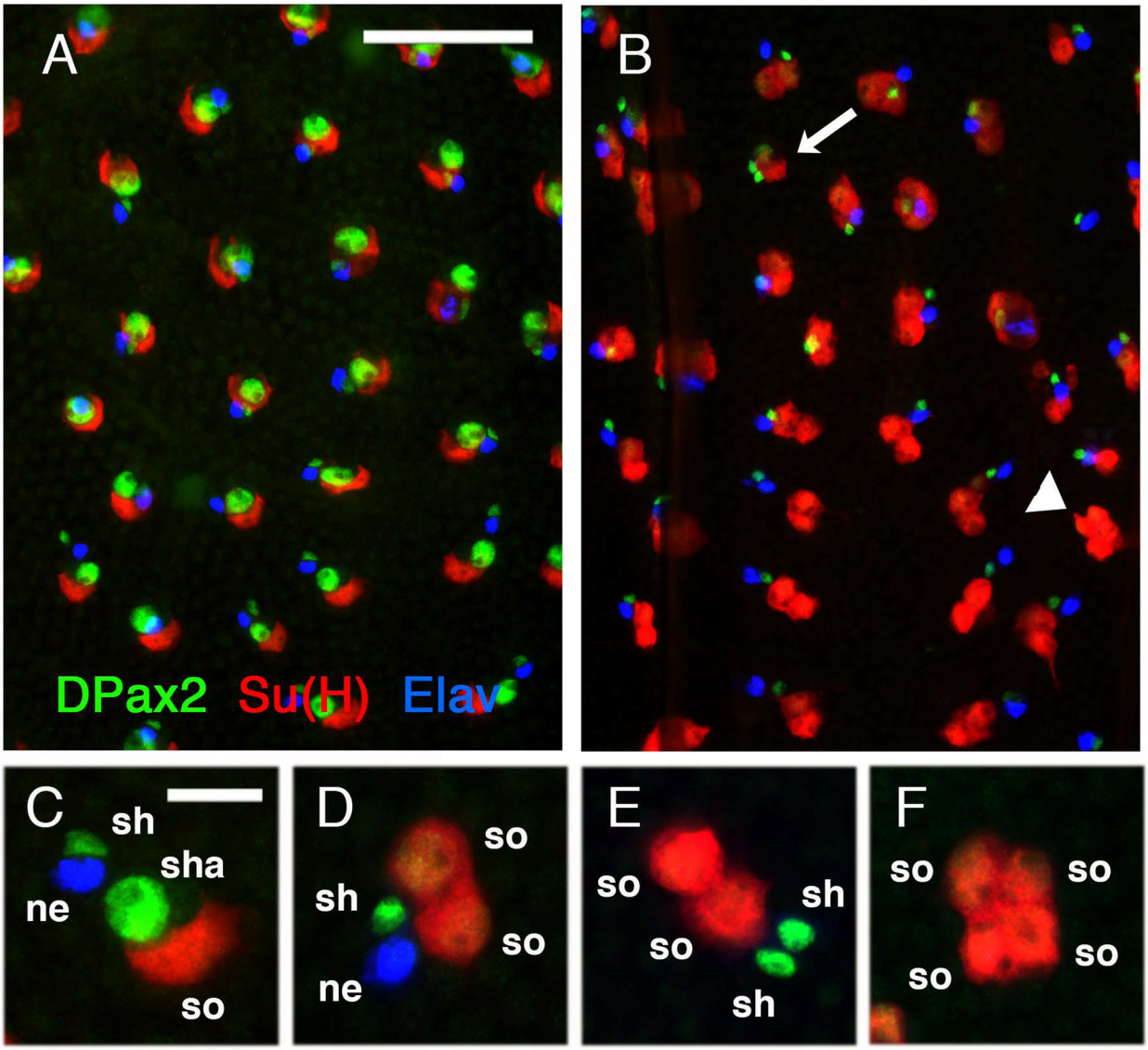

Figure 4.

CHMP2B^{Intron5} can cause cell fate transformations at several decision points in the ES organ lineage. Images of pupal nota from *neur>CHMP2B^{WT}* (A, C) and *neur>CHMP2B^{Intron5}* (B, D-F). Pupae were aged for 20 hours at 20°C and then shifted to 29°C for 12 hours to release GAL80 repression. Pupae were then placed back at 20°C for another 12–14 hours, followed by dissection and staining. Developmental stage of pupae at time of staining is approximately equivalent to a 30–32 hour APF pupa raised at 25°C. Staining included anti-DPax2 (green) which marks the large shaft cell nucleus (sha) and small sheath cell nucleus (sh), anti-Su(H) which marks the socket cell nucleus (so), and anti-Elav which marks the neuron nucleus (ne). White bar for panels A and B represents 50 μm. White bar for panels C-F represents 10 μm.

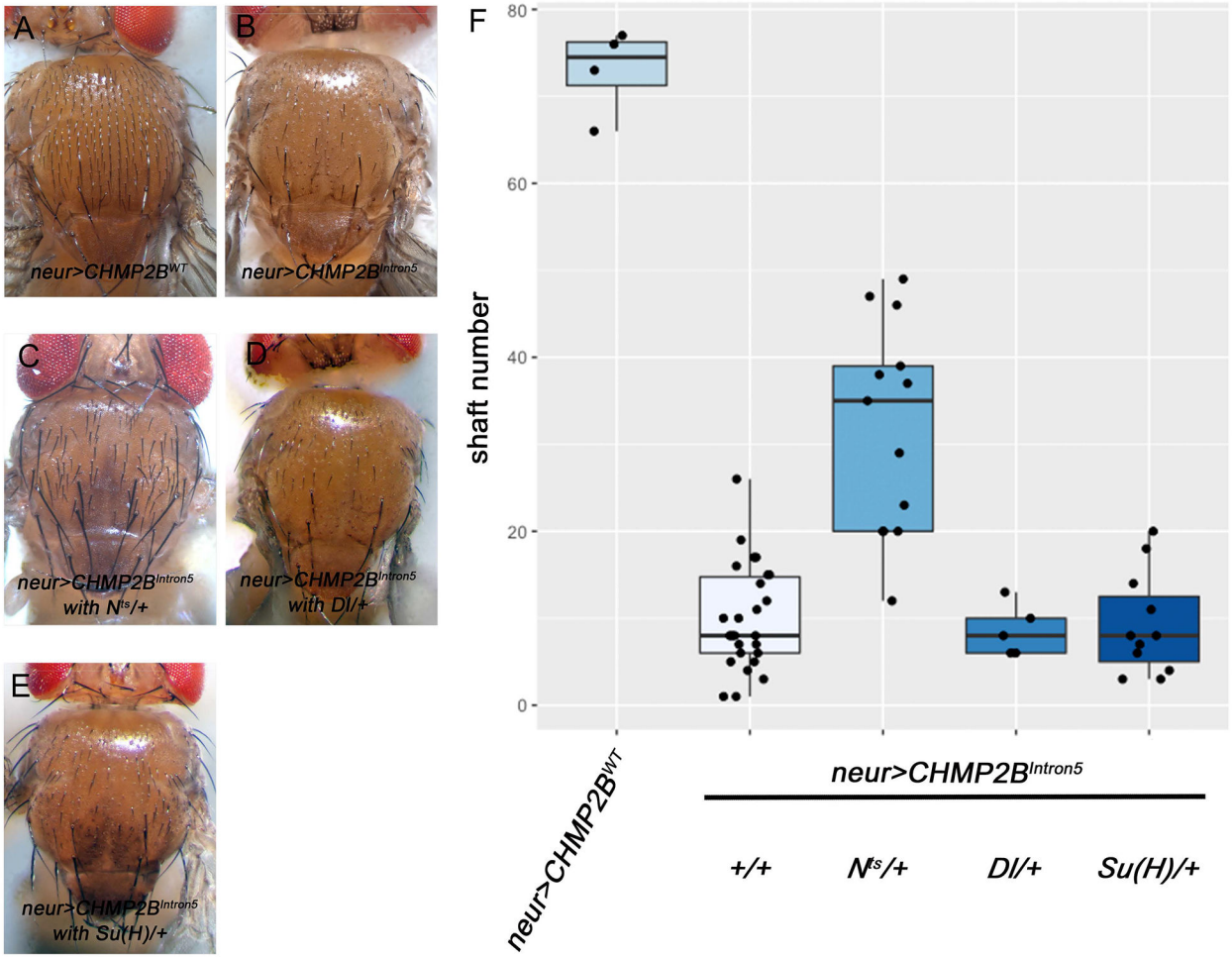

Figure 5.

Effect of decreased Notch dosage on shaft loss phenotype. Images of dorsal thoraces of the following flies: A) *neur>CHMP2B*^{WT}, B) *neur>CHMP2B*^{Intron5}, C) *neur>CHMP2B*^{Intron5} in *N*^{ts}*/+* background, D) *neur>CHMP2B*^{Intron5} in *Dl/+* background, E) *neur>CHMP2B*^{Intron5} in *Su(H)/+* background. F. Boxplot depicting quantification of shafts on the central region of the thorax. Lower and upper boundaries of the box mark the 25th and 75th percentile with the black line marking the median. The whiskers delineate the complete range of values. Welch's two-sample t-tests were conducted for each pair of genotypes and indicated statistically significant differences in shaft number between the genotypes. P-values for *neur>CHMP2B*^{WT} versus *neur>CHMP2B*^{Intron5}, *neur>CHMP2B*^{Intron5} versus *neur>CHMP2B*^{Intron5} in *N*^{ts}*/+* background and *neur>CHMP2B*^{WT} versus *neur>CHMP2B*^{Intron5} in *N*^{ts}*/+* background were 8.12e-06, 1.73e-05, and 2.07e-07 respectively. P-values for *neur>CHMP2B*^{Intron5} alone versus in *Dl/+* or *Su(H)/+* background were 0.458 and 0.749 respectively

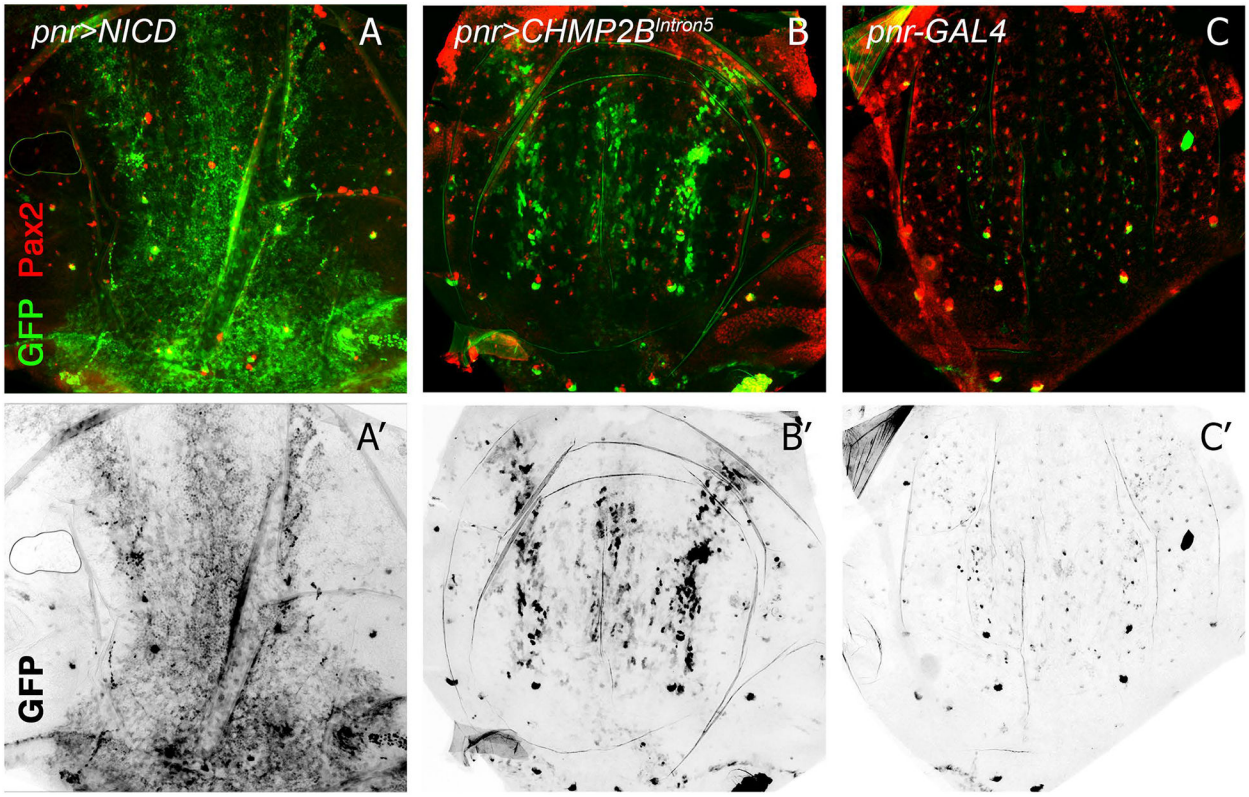

Figure 6.

CHMP2B^{Intron5} expression is associated with increased Notch activity. Images of pupal nota from *pnr>NICD* (A, A'), *pnr>CHMP2B^{Intron5}* (B, B'), and *pnr-Gal4* alone (C, C') flies which also contain *NRE-GFP*. In the top panels, GFP is shown in green and DPax2 staining is shown in red to demarcate the bristle positions. Pupae were aged 12 hours at 20°C and then shifted to 29°C for 14 hours to release GAL80 repression. Pupae were then dissected and stained for DPax2. Bottom panels are inverted grayscale images of the green channel by itself to highlight the GFP expression pattern. Scale bar in Panel A represents 100 μm.